Electric Dipole Moments in a General Two Higgs Doublet Model

Sven Teunissen

Advisor: Wei-Shu Hou

Graduate Institute of Physics

National Taiwan University

Taipei, Taiwan

June 2024

Abstract

The Standard Model (SM) of particle physics has been the dominant theory of all fundamental physics sans gravity for a good 50-or-so years. The SM provides a unifying mathematical framework, explanations for various atomic and subatomic phenomena, and a plethora of predictions, many of which have since been verified by experiments to high precision. Nevertheless, there are still questions the SM still does not have an answer for, one of them being the imbalance of naturally existing matter and antimatter, also known as the Baryon Asymmetry of the Universe (BAU). Motivated by this question (among others), there have been various theoretical attempts at extending beyond the Standard Model (BSM). One family of these extensions are the Two-Higgs Doublet Models (2HDMs), which propose an extra Higgs doublet with varying properties. Among these 2HDMs, one type does not have any assumed symmetry or coupling constraints, and is known as the General Two Higgs Doublet Model (G2HDM). A key feature of such theories attempting to address BAU is large charge-parity violation (CPV). On the experimental front, both the lack of new collider observations as well as the smallness of low-energy precision measurements put heavy constraints on BSM CPV. In particular, the electric dipole moments (EDMs) of various fundamental particles provide a *litmus test* for CPV effects. This study is an examination and analysis of various EDMs under the G2HDM framework. We start with the electron EDM (eEDM), introducing a *cancellation mechanism* that allows for an adequate parameter space to address the BAU issue while evading the current EDM bounds. We then extend the framework to the muon and the tau, and present both general

and cancellation-imposed results for the EDM of heavier leptons. We also probe the effects of the light quark EDMs through the neutron EDM (nEDM), taking into account gluon-related contributions. At last, we present a combined scenario analysis of the eEDM and the nEDM, signifying that experimental verification, or even *discovery*, is achieveable within the next decade or two.

Contents

List of Figures

List of Tables

Chapter 1

Introduction

One of the biggest unanswered questions of particle physics is that of baryogenesis. Specifically, if electroweak baryogenesis (EWBG) [**?**] were to occur, one would require very large CP violation (CPV) beyond the Standard Model (BSM), since the SM currently houses all its CPV in the CKM matrix [2]. However, such large BSM-CPV should have led to new discoveries at the LHC, which evidently is *not* what has been observed. Moreover, in the low-energy precision frontier, electric diploe moments (EDMs) provide a *litmus test* for CPV effects, and experiments have achieved higher and higher precision without discoveries, setting ever more stringent bounds.

1.1 The Standard Model of Particle Physics

The current working theory in the realm of particle physics is the Standard Model (SM).

1.2 Limits of the Standard Model

The SM is a powerful theory, providing a unifying framework for three of the four fundamental forces, and producing many verified predictions. However, it is clear

that the SM is *definitely not* the ultimate framework, and there is definitely room for extensions and modifications. To quote from the textbook *Modern Particle Physics* by Mark Thomson [3], "[The Standard Model] is a model constructed from a number of beautiful and profound theoretical ideas put together in a somewhat *ad hoc* fashion in order to reproduce the experimental data." Amidst all its strength, there are still several open questions that the SM has not been able to answer. In particular, the baryon asymmetry of the universe (BAU) problem is about the observed imbalance in baryonic matter and anti-baryonic matter amounts. Current cosmological theory predict that the Big Bang started with an almost equal number of quarks and antiquarks [4]. It is further hypothesized that during the expansion and cooling of the universe, some physical process occured that created the observed BAU. This process is known as baryogenesis [5] (formerly baryosynthesis [6, 7]). In particular, electroweak baryogenesis (EWBG) is the theory where such a baryogenesis process takes place during the electroweak phase transition (EWPT) [8, 9]. Inspired by the discoveries of the Cosmic Microwave Background (CMB) [10] and CPV in the neutral Kaon system [11], Andrei Sakharov proposed [12] a set of three necessary conditions for BAU, and consequentially baryogenesis, to occur:

1. Baryon number B violation.
2. C- and CP-symmetry violation.
3. Deviation from thermal equilibrium.

Baryon number violation is necessary to produce an excess amount of baryons in an interaction. C-symmetry violation is necessary so that interactions that produce and excess amount of baryons will not be balanced by interactions that produce an excess amount of anti-baryons. CPV is necessary otherwise equal numbers of left-handed baryons and right-handed anti-baryons would be produced, as well as equal numbers of left-handed anti-baryons and right-handed baryons. Deviation from thermal equilibrium is necessary otherwise CPT symmetry would assure compensation between processes increasing and decreasing the baryon

number [13]. The SM does not have an adequate amount of CP violation to account for the observed asymmetry, nor does it have out-of-equilibrium processes. However, with two or more Higgs doublets, EWBG is achieveable [14], with the added bonus that the proposed sub-TeV dynamics can be tested at the LHC. This motivates us to consider models that are SM extensions featuring two Higgs doublets, also known as two Higgs doublet models (2HDMs).

Chapter 2

The General Two-Higgs Doublet Model

There have been a plethora of 2HDMs proposed throughout the years, each model with its own set of additional assumptions. A comprehensive review of various 2HDMs can be found in [15].

2.1 The Model

Following Gell-Mann's *Totalitaian principle*, as a natural extension to the SM, we can introduce a second Higgs doublet. This second doublet couples to all flavors and families of fermions, and has no symmetry requirement imposed upon it. Hence, it is referred to as the "General Two Higgs Doublet Model", or G2HDM for short.

The G2HDM Lagrangian can be written as [**?**, **?**]

$$\mathcal{L} = -\frac{1}{\sqrt{2}} \sum_{f=u,d,\ell} \bar{f}_i \Big[\Big(-\lambda_i^f \delta_{ij} s_\gamma + \rho_{ij}^f c_\gamma \Big) h + \Big(\lambda_i^f \delta_{ij} c_\gamma + \rho_{ij}^f s_\gamma \Big) H - i\,\mathrm{sgn}(Q_f) \rho_{ij}^f A \Big] R\, f_j$$
$$-\bar{u}_i \left[(V\rho^d)_{ij} R - (\rho^{u\dagger} V)_{ij} L \right] d_j H^+ - \bar{\nu}_i \rho_{ij}^L R\, \ell_j H^+ + \mathrm{h.c.}, \tag{2.1}$$

where the generation indices i, j are summed over, L, $R = (1 \pm \gamma_5)/2$ are projections, V is the CKM matrix for quarks and unity for leptons. λ^f are the

SM Yukawa matrices, and ρ^f are the extra-Yukawa matrices. A key takeaway is that each family of fermions (u-type, d-type, lepton) is associated with its own extra-Yukawa ρ matrix. In this scenario, flavor-changing neutral Higgs (FCNH) processes are controlled by *flavor hierarchies* and *alignment*. Flavor hierarchies means that the ρ matrices somehow "know" the current flavor structure of the SM, represented by the "rule of thumb" [**?**]

$$\rho_{ii} \lesssim \mathcal{O}(\lambda_i), \quad \rho_{1i} \lesssim \mathcal{O}(\lambda_1), \quad \rho_{3j} \lesssim \mathcal{O}(\lambda_3), \tag{2.2}$$

with $j \neq 1$. Alignment means that $c_\gamma \equiv \cos\gamma = \cos(\beta - \alpha)$ is small. Consequently, the SM-like Higgs h is mostly controlled by the SM Yukawas, while the newly introduced ρ matrices control the exotic Higgses $H, A, H^\pm$. A remarkable feature of G2HDM is that $\mathcal{O}(1)$ ρ_{tt} can drive EWBG through [16] $\lambda_t \mathrm{Im}\rho_{tt}$.

2.2 Electroweak Baryogenesis

Even though the SM Lagrangian is baryon number conserving, there still is the possibility of baryon-number-violating processes due to a quantum anomaly [17]. This anomaly gives rise to baryon-number-violating but $(B - L)$ conserving sphaleron transitions [18], where B is baryon number and L is lepton number. The rate of these transitions Γ_B scale with temperature as $\sim \exp\left[-\frac{\pi m_W(T)}{\alpha_W}\right]$ [8], with m_W the W boson mass and α_W the weak coupling constant, which means that said transitions are more rapid in the earlier symmetric phase of the universe, before the symmetry breaking phase transition that induces the Higgs vev occurs. If Γ_B is larger than the expansion rate of the universe, namely the Hubble parameter H, then any "primordial" baryon asymmetry will be washed out by these sphaleron processes. This implies that the EWPT must be a first-order phase transition, and that the vev aquired in the broken phase must be large enough such that $\Gamma_B^{(\mathrm{br})}(T_C) < H(T_C)$ at critical temperature T_C. This ensures that any baryon asymmetry generated by *the phase transition itself* will persist without being washed out. During this phase transition, "bubbles" of the new broken phase

nucleate and expand to fill the universe [19]. This creates a departure from thermal equilibrium, satisfying the third Sakharov condition. If there exists CPV in the particle interactions that happen at the bubble walls, then BAU can be generated. Unfortunately, as mentioned before, the CPV present in the SM is insufficient to drive the BAU of our current observable universe.

In G2HDM, we have an extra Higgs doublet, as well as extra Yukawa couplings to work with. Thermal loops of heavy Higgs bosons can create a strong enough first-order EWPT [14] to satisfy the above criteria, doing to $\mathcal{O}(1)$ nondecoupled [20] Higgs couplings. We can estimate BAU by [21, 22]

$$Y_B \equiv \frac{n_B}{s} = \frac{-3\Gamma_B^{(\mathrm{sym})}}{2D_q\lambda_+ s}\int_{-\infty}^{0} \mathrm{d}z'\, n_L(z')e^{-\lambda_- z'} \tag{2.3}$$

where $D_q \simeq 8.9/T$ is the quark diffusion constant, s is the entropy density, $\Gamma_B^{\mathrm{sym}} = 120\alpha_W^5 T$ is the B-changing rate in the symmetric phase, and $\lambda_\pm = [v_w \pm (v_w^2 + 15\Gamma_B^{\mathrm{sym}} D_q)^{1/2}]/2D_q$, with v_w the bubble wall velocity. The integration happens over z', which is the coordinate opposite of the bubble wall expansion direction. For Y_B to be nonzero, a nonvanishing total left-handed fermion number density n_L is needed. The current observational value $Y_B^{\mathrm{obs}} = 8.59 \times 10^{-11}$ comes from the Planck collaboration [23]. The BAU-related CPV arises from the interaction between particles/antiparticles with the bubble wall. As a result of their thermal motion, particles and antiparticles in the neighborhood of the bubble wall propagate through it. Since one side of the bubble wall has zero vev, while the other side has nonzero vev, the particles see the bubble wall as a potential barrier and scatter from it. A dominant process is shown in Figure 2.1. The Higgs bubble wall is denoted as $v_a(x)$, $v_b(y)$, which are spacetime-dependent vevs. The CPV source term S_{ij} for left-handed fermion f_{iL} induced by right-handed fermion f_{jR} in G2HDM is [16]

$$S_{iLjR}(Z) = N_C F \mathrm{Im}[(Y_1)_{ij}(Y_2)^*_{ij}]v^2(Z)\partial_{t_Z}\beta(Z) \tag{2.4}$$

where $Z = (t_Z, 0, 0, z)$ is the position in the heat bath, $N_C = 3$ is the number of color, and F is a function (see Ref. [24]). Essentially, the CPV for BAU is

contained in $\mathrm{Im}[(Y_1)_{ij}(Y_2)^*_{ij}]$. Diagonalizing gives

$$\mathrm{Im}[(Y_1)_{tc}(Y_2)^*_{tc}] = -\lambda_t \mathrm{Im}\rho_{tt}\,, \quad \rho_{tc} = 0 \tag{2.5}$$

And thus we arrive at the most important result of [16]: BAU can be driven in the G2HDM by $-\lambda_t \mathrm{Im}\rho_{tt}$.

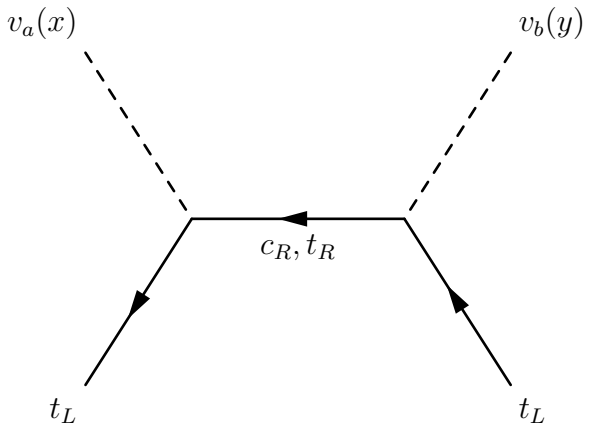

Figure 2.1: A dominant CPV process relevant for baryon asymmetry, with Higgs bubble wall denoted $v_a(x)$ and $v_b(y)$.

Chapter 3

Electric Dipole Moment

3.1 The electric dipole moment in particle physics

Classically, the electric dipole moment of a charge distribution is found as the coefficient of the $l = 1$ term in the multipole expansion of the potential of said distribution. Explicitly, it is[1]

$$\mathbf{d} = \int (\mathbf{r} - \mathbf{r}_0)\rho(\mathbf{r})\, \mathrm{d}^3\mathbf{r} \tag{3.1}$$

with $\mathbf{r}_0$ the center of mass of the charge distribution [25, 26]. It is related to the seperation of charges or nonuniformity along a single axis in the charge distribution; for a distribution of nonzero net charge, it is also related to the position of the center of mass with respect to the origin. It is inherently a property of systems of finite size[2]. However, in particle physics, we are not dealing with composite systems, but the properties of the fundamental particles. That means we are instead looking for an *intrinsic* EDM of point-like particles that is attributed to the particle itself, and not a seperation of charges. This is analogous to the (spin) magnetic dipole moment being an *intrinsic* property and not a tiny loop of current. In particluar,

[1] In classical texts, the dipole moment is represented with the symbol $\mathbf{p}$. For the sake of consistency with the particle physics notation, I have chosen the symbol $\mathbf{d}$ instead.

[2] There are point-like "dipoles" etc. in the classical framework, but they are purely mathematical and are not attributed to any physical thing.

particle physicists are interested in the EDMs of various fermions, since they are the point-like building blocks of all matter. Generally speaking, there are two ways to introduce this "EDM term", approaching the issue from slightly different angles.

3.1.1 The Dirac method

The first method is that of Dirac. In his 1928 paper [27], which gave birth to his famous Dirac equation, he also wrote down the equation for the electron in an arbitrary electromagnetic field. Adapted into more modern notation, it is written as

$$\left[-(E-e\phi)+\boldsymbol{\alpha}\cdot(\mathbf{p}-e\mathbf{A})+\beta m\right]\psi=0 \tag{3.2}$$

where

$$\alpha_i=\gamma^5\Sigma_i=\begin{pmatrix}0 & I\\ I & 0\end{pmatrix}\begin{pmatrix}\sigma_i & 0\\ 0 & \sigma_i\end{pmatrix}=\begin{pmatrix}0 & \sigma_i\\ \sigma_i & 0\end{pmatrix},\quad \beta=\begin{pmatrix}I & 0\\ 0 & -I\end{pmatrix} \tag{3.3}$$

in the Pauli-Dirac representation. By "squaring" (3.2) one obtains

$$\begin{aligned}&\left[(E-e\phi)+\boldsymbol{\alpha}\cdot(\mathbf{p}-e\mathbf{A})+\beta m\right]\left[-(E-e\phi)+\boldsymbol{\alpha}\cdot(\mathbf{p}-e\mathbf{A})+\beta m\right]\psi=0\\ \Longrightarrow&\Big[-(E-e\phi)^2+(\boldsymbol{\Sigma}\cdot(\mathbf{p}-e\mathbf{A}))^2+m^2\\ &\quad+\gamma^5\left\{(E-e\phi)(\boldsymbol{\Sigma}\cdot(\mathbf{p}-e\mathbf{A}))-(\boldsymbol{\Sigma}\cdot(\mathbf{p}-e\mathbf{A}))(E-e\phi)\right\}\Big]\psi=0\end{aligned} \tag{3.4}$$

After some matrix algebra, in particular $(\boldsymbol{\Sigma}\cdot\mathbf{a})(\boldsymbol{\Sigma}\cdot\mathbf{b})=(\mathbf{a}\cdot\mathbf{b})I+i\boldsymbol{\Sigma}\cdot(\mathbf{a}\times\mathbf{b})$, and casting E and $\mathbf{p}$ back into their operator forms when necessary, we arrive at

$$\Big[-(E-e\phi)^2+(\mathbf{p}-e\mathbf{A})^2+m^2-e\boldsymbol{\Sigma}\cdot\mathbf{B}-ie\gamma^5\boldsymbol{\Sigma}\cdot\mathbf{E}\Big]\psi=0 \tag{3.5}$$

which introduces two additional terms, corresponding to the magnetic and the electric dipole moment of the electron, respectively. At the time, Dirac thought the EDM term was merely a consequence of the "squaring" used in the derivation arbitrarily introducing an imaginary term from a real Hamiltonian, and disregarded it. It was only until 1958 when Salpeter [28] reintroduced this term in an "interaction Lagrangian" point of view [3].

[3] I discovered this fact through [29].

3.1.2 Form factor decomposition

The second method is based on form factor decomposition. This method was recently seen in [30]. We start by expressing the expectation value of the electromagnetic 4-current in momentum space as

$$\langle p_f|j^\mu|p_i\rangle = \bar{u}(\mathbf{p_f})\mathcal{O}^\mu(l,q)u(\mathbf{p_i}) \tag{3.6}$$

where $l \equiv p_f + p_i$ is the total 4-momentum, $q \equiv p_f - p_i$ is the momentum transfer, and $\mathcal{O}^\mu(l,q)$ is an operator whose matrix element between the spinors is a Lorentz vector. We then want to decompose $\mathcal{O}^\mu(l,q)$ in terms of the Clifford algebra of the Dirac gamma matrices. After identifying all possible combinations and contractions of $\left\{q^\mu, l^\mu, \gamma^\mu, \gamma^5, \sigma^{\mu\nu}, \epsilon^{\mu\nu\alpha\beta}\right\}$, applying various Gordon-like identities, and imposing gauge invariance[4] $q_\mu j^\mu = 0$, we arrive at four independent terms

$$\begin{aligned}
&\bar{u}(\mathbf{p_f})\mathcal{O}^\mu(l,q)u(\mathbf{p_i}) \\
&= \bar{u}(\mathbf{p_f})\left\{F_1(q^2)\gamma^\mu + \frac{i\sigma^{\mu\nu}}{2m}q_\nu F_2(q^2)\right. \\
&\qquad \left. +(-\gamma^5\sigma^{\mu\nu}q_\nu)\frac{1}{4m}F_3(q^2) + \frac{1}{2m}\left(q^\mu - \frac{q^2}{2m}\gamma^\mu\gamma^5\right)F_4(q^2)\right\}u(\mathbf{p_i})
\end{aligned} \tag{3.7}$$

We then couple this with the electromagnetic potential A_μ to obtain some physical insight on this result. Taking the non-relativistic limit ($q^2 = 0$), we can identify

$$F_1(0) = Q, \quad \frac{1}{2m}\left(F_1(0) + F_2(2)\right) = \mu, \quad -\frac{1}{2m}F_3(0) = d \tag{3.8}$$

are the charge, magnetic dipole moment, and electric dipole moment, respectively. Transforming the coupled current plus EM field back into position space, we can obtain the addition to the interaction Lagranginan for each term as well.

[4] Note that without gauge invariance imposed, there ought to be six independent terms, which is the case for the Weak current.

3.1.3 General properties of EDM

Regardless of approach, the end result, in terms of quantum field theory, is the inclusion of an effective dimension-5 interaction operator to the EM Lagrangian,

$$-\frac{i}{2}d_f\left(\bar{f}\sigma^{\mu\nu}\gamma_5 f\right)F_{\mu\nu}. \tag{3.9}$$

that produces EDM d_f for a fermion f, where $F_{\mu\nu}$ is the electromagnetic field strength tensor. If we examine the EDM term under the lens of discrete symmetry transformations, we can see that

$$\begin{aligned} \mathbf{E} &\xrightarrow{P} -\mathbf{E} \qquad \mathbf{E} \xrightarrow{T} \mathbf{E} \\ \mathbf{\Sigma} &\xrightarrow{P} \mathbf{\Sigma} \qquad \mathbf{\Sigma} \xrightarrow{T} -\mathbf{\Sigma} \end{aligned} \tag{3.10}$$

for parity transformation P and time-reversal transformation T. Thus, a nonzero EDM of fundamental particles indicates that both time-reversal and parity invariance are broken.

3.2 G2HDM contributions to EDMs

3.2.1 One-loop v.s. Two-loop

In G2HDM, the first finite contribution to EDM appears at one-loop (Figure 3.1). If we look at the figure, there are two Yukawa interaction vertices along the fermion line. Each Yukawa interaction vertex flips the chirality of the fermion. In the previous section we observed that the dipole operator breaks parity invariance, and thus is chirality violating. Since the only chirality-flipping vertices along the fermion line are the Yukawa interaction vertices, we need an extra chirality flip somewhere along the line to obtain the correct chiral structure. This is achieved by requiring an additional mass insertion on the fermion line, i.e. treating the small mass of the fermion as an "interaction" between the (massless) chiral states. Since the mass of the fermions in question are very small, both the Yukawa vertices and the mass insertion effectively suppress the amplitude of the one loop-diagrams.

This is known as "chiral suppression", and opens the possibility of two-loop diagrams making meaningful contributions.

A certain set of two-loop diagrams, known as Barr-Zee diagrams (Figure 3.2), are indeed of importance. These diagrams were first mentioned by Bjorken and Weinberg [31], but it was Barr and Zee [32] that calculated neutral scalar contributions with top quark and gauge bosons in the loop. This was later extended [33, 34, 35, 36, 37] to include other two-loop diagrams. These diagrams only contain one Yukawa interaction vertex, hence one chirality flip, as opposed to three in the one-loop case. The relative enhancement due to the lack of the two mass factors more than compensate for the suppression from the additional loop factor. Thus, interestingly, the two-loop diagrams become the dominant contribution to the EDM interaction operator.

3.2.2 Two-loop Formulae

In this subsection, we list all the relevant formulae involved in the calculation of the two-loop Barr-Zee diagram amplitudes with different loop particles. The formulae are compiled from various resources, and verified by us before using them. We also explicitly draw out all of the corresponding diagrams in Figure 3.3. The formulae for the neutral-Higgs-mediated diagrams are taken from [37]; The formulae for the charged-Higgs-mediated diagrams are taken from [36, 37]. The notation follows that of [37].

$$(d_l^{\phi G})_t = -\frac{e\, m_l}{(4\pi)^4}\sqrt{2}G_F \sum_{\phi=h,H,A}\sum_{G=\gamma,Z} N_c Q_t (g^L_{Gll} + g^R_{Gll}) \times \left[\frac{g^A_{\phi ll}}{m_l/v}\frac{g^V_{\phi tt}}{m_t/v}\mathcal{I}_1^G(m_t, m_\phi) + \frac{g^V_{\phi ll}}{m_l/v}\frac{g^A_{\phi tt}}{m_t/v}\mathcal{I}_2^G(m_t, m_\phi)\right] \quad (3.11)$$

where

$$\mathcal{I}_1^G(m_t, m_\phi) = (g_{Gtt}^L + g_{Gtt}^A)\frac{m_t^2}{m_\phi^2 - m_G^2}\left(-2\frac{m_G^2}{m_t^2}f\left(\frac{m_t^2}{m_G^2}\right) + 2\frac{m_\phi^2}{m_t^2}f\left(\frac{m_t^2}{m_\phi^2}\right)\right)$$
$$\mathcal{I}_2^G(m_t, m_\phi) = (g_{Gtt}^L + g_{Gtt}^A)\frac{m_t^2}{m_\phi^2 - m_G^2}\left(-2\frac{m_G^2}{m_t^2}g\left(\frac{m_t^2}{m_G^2}\right) + 2\frac{m_\phi^2}{m_t^2}g\left(\frac{m_t^2}{m_\phi^2}\right)\right) \tag{3.12}$$

$$(d_l^{\phi G})_W = +\frac{e\, m_l}{(4\pi)^4}\sqrt{2}G_F \sum_{\phi=h,H,A}\sum_{G=\gamma,Z}(g_{Gll}^L + g_{Gll}^R)\frac{g_{\phi ll}^A}{m_l/v}\frac{g_{WW\phi}}{2m_W^2/v}\mathcal{I}_W^G(m_\phi) \tag{3.13}$$

where

$$\begin{aligned}\mathcal{I}_W^G(m_\phi) =& g_{WWG}\frac{2m_W^2}{m_\phi^2 - m_G^2} \\ &\times\left[-\frac{1}{4}\left\{\left(6 - \frac{m_G^2}{m_W^2}\right) + \left(1 - \frac{m_G^2}{2m_W^2}\right)\frac{m_\phi^2}{m_W^2}\right\}\left[-2\frac{m_\phi^2}{m_W^2}f\left(\frac{m_W^2}{m_\phi^2}\right) + 2\frac{m_G^2}{m_W^2}f\left(\frac{m_W^2}{m_G^2}\right)\right]\right. \\ &\left.+\left\{\left(-4 + \frac{m_G^2}{m_W^2}\right) + \frac{1}{4}\left(\left(6 - \frac{m_G^2}{m_W^2}\right) + \left(1 - \frac{m_G^2}{2m_W^2}\right)\frac{m_\phi^2}{m_W^2}\right)\right\}\left[-2\frac{m_\phi^2}{m_W^2}g\left(\frac{m_W^2}{m_\phi^2}\right) + 2\frac{m_G^2}{m_W^2}g\left(\frac{m_W^2}{m_G^2}\right)\right]\right]\end{aligned} \tag{3.14}$$

$$(d_l^{\phi G})_{H^\pm} = +\frac{e\, m_l}{(4\pi)^4}\sqrt{2}G_F \sum_{\phi=h,H,A}\sum_{G=\gamma,Z}(g_{Gll}^L + g_{Gll}^R)\frac{g_{\phi ll}^A}{m_l/v}\frac{g_{\phi H^+H^-}}{v}\mathcal{I}_3^G(m_{H^\pm}, m_\phi) \tag{3.15}$$

where

$$\begin{aligned}\mathcal{I}_3^G(m_{H^\pm}, m_\phi) =& -\frac{1}{2}g_{GH^+H^-}\frac{v^2}{m_\phi^2 - m_G^2} \\ &\times\left[\left(-2\frac{m_G^2}{m_{H^\pm}^2}f\left(\frac{m_{H^\pm}^2}{m_G^2}\right) + 2\frac{m_\phi^2}{m_{H^\pm}^2}f\left(\frac{m_{H^\pm}^2}{m_\phi^2}\right)\right) - \left(-2\frac{m_G^2}{m_{H^\pm}^2}g\left(\frac{m_{H^\pm}^2}{m_G^2}\right) + 2\frac{m_\phi^2}{m_{H^\pm}^2}g\left(\frac{m_{H^\pm}^2}{m_\phi^2}\right)\right)\right]\end{aligned} \tag{3.16}$$

$$(d_l^{H^+W^+})_{t/b} = -\frac{3em_l}{(4\pi)^4}\frac{m_w^2}{v^4}\left(\frac{v^2}{2m_t m_l}\mathrm{Im}\rho_{tt}\rho_{ll}\Big(Q_t F_t(m_{H^\pm}) + Q_b F_b(m_{H^\pm})\Big)\right) \tag{3.17}$$

where

$$F_q(m_{H^\pm}) = \frac{T_q(m_{H^\pm}^2/m_t^2) - T_q(m_W^2/m_t^2)}{(m_{H^\pm}^2/m_t^2) - (m_W^2/m_t^2)} \tag{3.18}$$

$$(d_l^{H^+W^+})_W = -\frac{em_l}{(4\pi)^4}\sqrt{2}G_F\mathcal{S}_l \sum_h \frac{g_{llh}^A}{m_l/v}\frac{g_{WWh}}{2m_W^2/v}\frac{e^2}{2s_W^2}\mathcal{I}_4(m_h, m_{H^\pm}) \tag{3.19}$$

where

$$\mathcal{I}_4(m_h, m_{H^\pm}) = \frac{m_W^2}{m_{H^\pm}^2 - m_W^2}\Big[I_4(m_W, m_h) - I_4(m_{H^\pm}, m_h)\Big] \tag{3.20}$$

$$(d_l^{H^+W^+})_{H^+} = -\frac{em_l}{(4\pi)^4}\sqrt{2}G_F\mathcal{S}_l \sum_h \frac{g_{llh}^A}{m_l/v}\frac{g_{HHh}}{v}\frac{e^2}{2s_W^2}\mathcal{I}_5(m_h, m_{H^\pm}) \tag{3.21}$$

where

$$\mathcal{I}_5(m_h, m_{H^\pm}) = \frac{m_W^2}{m_{H^\pm}^2 - m_W^2}\Big[I_5(m_W, m_h) - I_5(m_{H^\pm}, m_h)\Big] \tag{3.22}$$

with loop functions

$$f(a) = \frac{1}{2}a\int_0^1 \mathrm{d}z\, \frac{1-2z(1-z)}{z(1-z)-a}\log\frac{z(1-z)}{a} \tag{3.23}$$

$$g(a) = \frac{1}{2}a\int_0^1 \mathrm{d}z\, \frac{1}{z(1-z)-a}\log\frac{z(1-z)}{a} \tag{3.24}$$

$$T_t(a) = \frac{1-3a}{a^2}\frac{\pi^2}{6} + \left(\frac{1}{a} - \frac{5}{2}\right)\log a - \frac{1}{a} - \left(1-\frac{1}{a}\right)\left(2-\frac{1}{a}\right)\mathrm{Li}_2(1-a) \tag{3.25}$$

$$T_b(a) = \frac{2a-1}{a^2}\frac{\pi^2}{6} + \left(\frac{3}{2} - \frac{1}{a}\right)\log a + \frac{1}{a} - \frac{1}{a}\left(1-\frac{1}{a}\right)\mathrm{Li}_2(1-a) \tag{3.26}$$

$$I_4(m_i, m_\phi) = \int_0^1 \mathrm{d}z\, \frac{m_i^2\left(z(1-z)^2 - 4(1-z)^2 + \frac{m_{H^\pm}^2 m_\phi^2}{m_W^2}z(1-z)^2\right)}{m_W^2(1-z) + m_\phi^2 z - m_i^2 z(1-z)}\log\left(\frac{m_W^2(1-z)+m_\phi^2 z}{m_i^2 z(1-z)}\right) \tag{3.27}$$

$$I_5(m_i, m_\phi) = 2\int_0^1 \mathrm{d}z\, \frac{m_i^2 z(1-z)^2}{m_{H^\pm}^2(1-z) + m_\phi^2 z - m_i^2 z(1-z)}\log\left(\frac{m_{H^\pm}^2(1-z)+m_\phi^2 z}{m_i^2 z(1-z)}\right) \tag{3.28}$$

3.3 Chromoelectric dipole moment

If we were only interested in lepton EDM, then the previous discussion would have been sufficient, since leptons only participate in the electroweak interaction. However, quarks also participate in the strong interaction, so there will be QCD-related effects. This can be found in two additional terms in the Lagrangian: the chromo-EDM $\tilde{d}_f$ for fermion f, and the Weinberg term C_W for gluon interactions [38], written as

$$-\frac{ig_s}{2}\tilde{d}_f\left(\bar{f}\sigma^{\mu\nu}T^a\gamma_5 f\right)G^a_{\mu\nu} \qquad -\frac{1}{3}C_W f^{abc}G^a_{\mu\sigma}G^{b,\sigma}_{\nu}\tilde{G}^{c,\mu\nu} \tag{3.29}$$

which correspond to the diagrams in Figure 3.4. The chromo-EDM term is essentially when the vector bosons of the "ordinary" EDM interaction are replaced by gluons instead. Since only quarks interact with gluons, only the diagram with a fermion loop remains. The Weinberg term is relevant because quarks always exist in bound hadronic states. That means experimentally we use the EDM of hadrons to infer about quark EDM, and thus the gluon interactions within the hadrons will contribute to the hadron EDM. We evaluate the contributions to $\tilde{d}_{u,d}$ and C_W in G2HDM by following Refs. [**?**] and [**?**], with discussion on theoretical uncertainties found in Ref. [**?**]. The formulae for calculating the cEDM are

$$\tilde{d}_f = +\frac{m_f}{(4\pi)^4}\sqrt{2}G_F\sum_{\phi=h,H,A}2g_s^2\frac{m_f^2}{m_\phi^2}\left[\frac{g^A_{\phi ff}}{m_f/v}\frac{g^V_{\phi tt}}{m_t/v}\left(-2\frac{m_\phi^2}{m_t^2}f\left(\frac{m_t^2}{m_\phi^2}\right)\right)+\frac{g^V_{\phi ff}}{m_f/v}\frac{g^A_{\phi tt}}{m_t/v}\left(-2\frac{m_\phi^2}{m_t^2}g\left(\frac{m_t^2}{m_\phi^2}\right)\right)\right] \tag{3.30}$$

$$C_W = \tag{3.31}$$

The contribution of the Weinberg diagram can be evaluated using QCD running.

$$\frac{d_f(\mu_h)}{2} = \tag{3.32}$$

$$\frac{\tilde{d}_f(\mu_h)}{2} = \tag{3.33}$$

$$C_W(\mu_h) = \tag{3.34}$$

where constants.

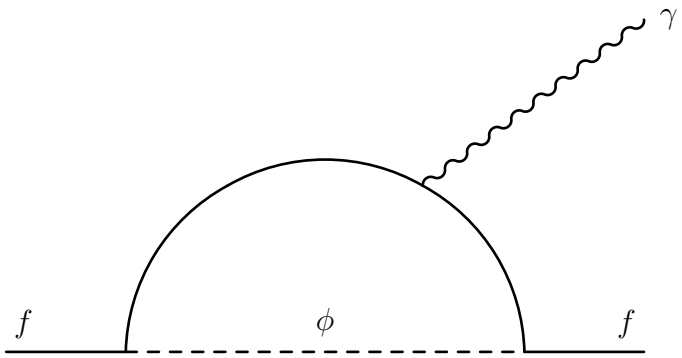

Figure 3.1: One-loop diagram

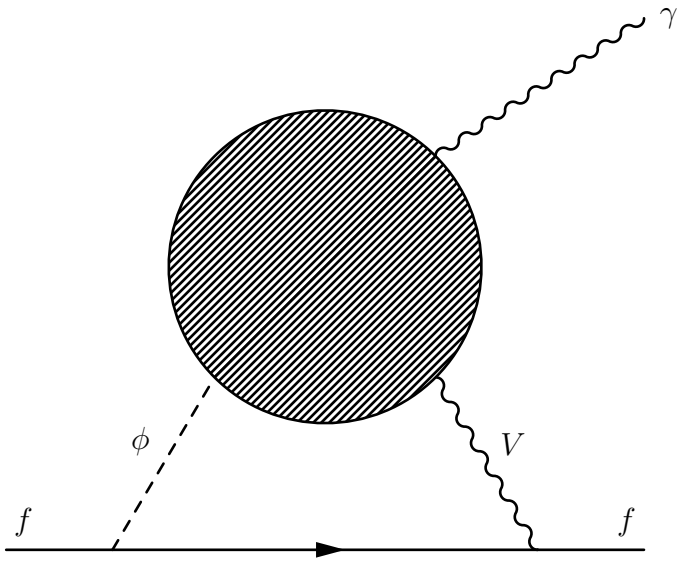

Figure 3.2: Two-loop Barr-Zee diagram

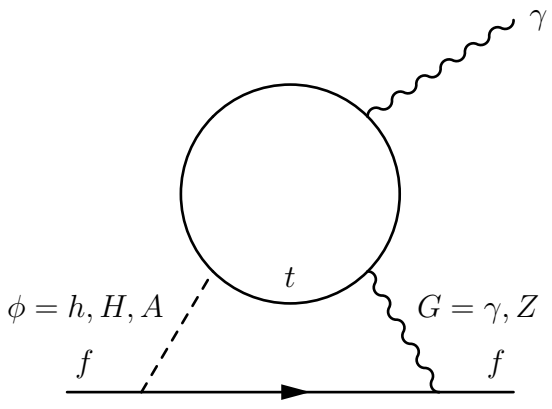

(a) Neutral Higgs, top loop

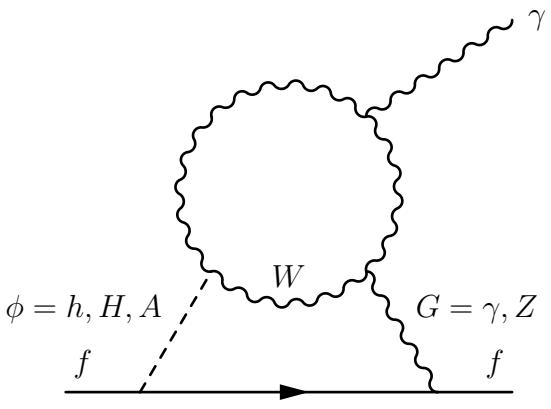

(b) Neutral Higgs, W loop

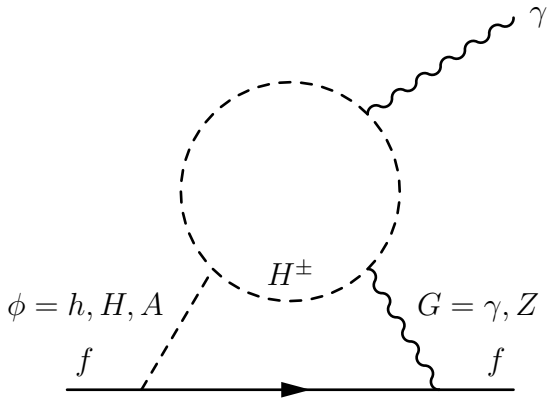

(c) Neutral Higgs, charged Higgs loop

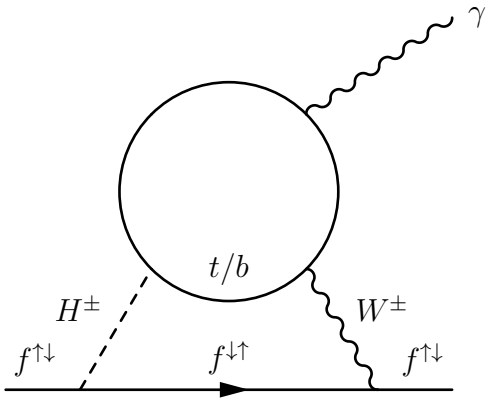

(d) Charged Higgs, top/bottom loop

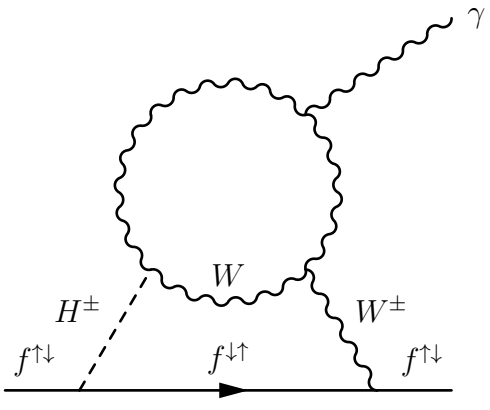

(e) Charged Higgs, W loop

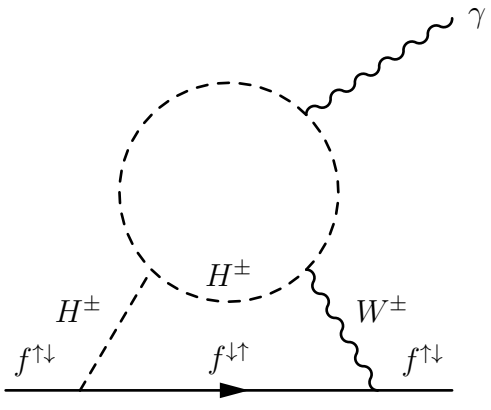

(f) Charged Higgs, charged Higgs loop

Figure 3.3: Specific Two-loop Barr-Zee diagrams

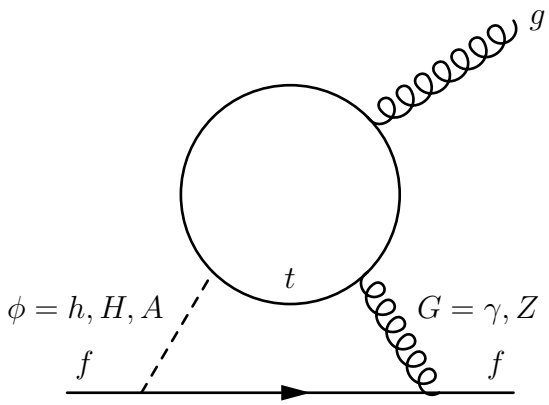

(a) Barr-Zee diagram, gluons

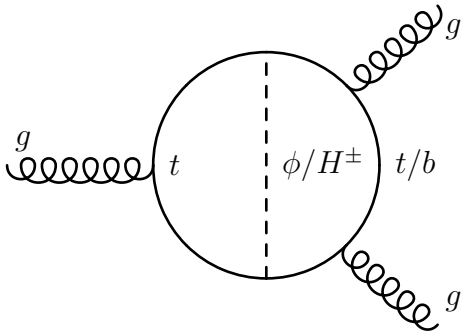

(b) Weinberg diagram

Figure 3.4: Diagrams relevant to chromo-EDM

Chapter 4

Electric Dipole Moment of Leptons

Following the framework laid out previously, we want to perform EDM calculations on the various leptons. However, we shall ignore the neutrinos. Thoretically, they are neutral and massless, thus they *at best* will receive EDM contributions from the charged-Higgs related processes, and are of lower theoretical significance. Experimentally, EDM experiments are low-energy in nature, and low-energy manipulation of neutrinos is currently experimentally unfeasable. We will thus focus our calculations on the electron and its cousins, the muon and the tau. Any subsequent mention of "leptons" in this work will also by default only be referring to these three leptons. In the following sections of this chapter, we will first give a brief overview of the current experimental status, then present our theoretical predictions of the EDMs of the electron, muon, and tau respectively.

4.1 Experimental Overview

A brief overview of current experimental bounds and projected future experimental sensitivity is given in Table 4.1.

As can be seen in the table, the experimental development of electron EDM (eEDM) over the past few years has been remarkably rapid. Just earlier in 2023, JILA [39] has surpassed the previous bound from ACME [40] and pushed the

Lepton	Current bound (e cm)		Future sensitivity (e cm)	
Electron	4.1×10^{-30}	JILA (2023) [39]		
	1.1×10^{-29}	ACME (2018) [40]		
Muon	1.8×10^{-19}	BNL (2009) [41]	$\sim 10^{-21}$	FNAL [42], J-PARC [43]
	$\sim 2 \times 10^{-20}$	Pospelov (2022) [44]	$\sim 6 \times 10^{-23}$	PSI [45]
Tau	$\mathrm{Re}\, d_\tau = -0.62(63) \times 10^{-17}$	Belle (2003) [46]	$\sim 10^{-18} - 10^{-19}$	Belle II [47]
			$\sim 0.7 \times 10^{-19}$	Bernreuther [48]
	$\mathrm{Im}\, d_\tau = -0.40(32) \times 10^{-17}$	Belle (2003) [46]	$\sim 10^{-18} - 10^{-19}$	Belle II [47]
			$\sim 0.4 \times 10^{-19}$	Bernreuther [48]

Table 4.1: Overview of current bounds and future sensitivities for lepton EDMs.

precision of eEDM down to $|d_e| < 4.1 \times 10^{-30}\ e\,\mathrm{cm}$. It is noteworthy to point out that these eEDM experiments are relatively small in scale, "tabletop experiments" even when compared to behemoths like the LHC, which makes the extreme precision achieved all the more impressive. The smallness of eEDM, courtesy of this precision, has put significant pressure on the theoretical side of baryogenesis CPV parameter spaces. In Section 4.2 we shall establish in G2HDM a way to maintain adequate baryogenesis efficiency while evading the experimental eEDM bounds.

For the muon, the leading experimental bound on muon EDM (μEDM) is by the Muon g-2 experiment at Brookhaven National Laboratory (BNL) [41], giving us the bound $|d_\mu| < 1.8 \times 10^{-19}\ e\,\mathrm{cm}$. There is also an indirect limit derived from the ACME 2018 eEDM bound, which is claimed [44] to be $\sim 2 \times 10^{-20}\ e\,\mathrm{cm}$. There are several experiments that aim to search for μEDM in the forseeable future. The Fermilab (FNAL) Muon g-2 [42] and J-PARC Muon g-2/EDM [43] experiments project their sensitivities at $\sim 10^{-21}\ e\,\mathrm{cm}$, while another experiment at PSI [45] aims to improve by an additional order of magnitude, reaching $\sim 6 \times 10^{-23}\ e\,\mathrm{cm}$. With these experiments on the horizon, the prospects for μEDM in the coming decade do look rather promising.

As for the tau, tau EDM (τEDM) measurements are far less precise given

the short lifetime of the tau lepton. The most prominent method to derive the limits are from spin-momentum correlations of final state decay products in the $e^+e^- \to \gamma^* \to \tau^+\tau_-$ process, where τEDM enters the matrix element of the $\tau\tau\gamma$ vertex. The current best limit is by Belle [46], with the real and imaginary parts given seperately, both at $\sim 10^{-17}$. Just as with μEDM, an indirect limit can be derived from eEDM as per [44] (not listed here). Belle II [47] projects an order-of-magnitude improvement to the Belle bounds. On the other hand, some improvement is possible by studying "optimal" observables, as per [48].

If we assume that new physics (NP) contributions scale with m_l (such as models [49] with minimal flavor violation (MFV)), we can make back-of-the-envelope estimates of the "equivalent precision" bounds for μEDM and τEDM from the current eEDM bound. Applying the scaling $|d_{\mu(\tau)}/d_e| \simeq m_{\mu(\tau)}/m_e$ to the JILA bound in Table 4.1, we can obtain the equivalent precision bounds $|d_\mu| \sim 8.5 \times 10^{-28}\ e\,\mathrm{cm}$ and $|d_\tau| \sim 1.4 \times 10^{-26}\ e\,\mathrm{cm}$, respectively. Referring back to Table 4.1, the projected sensitivities for μEDM fall just shy of 5 orders of magnitude short, while those for τEDM are still st least 7 orders of magnitude away. However, if the flavor dynamics are quite different, this m_l scaling might not hold [50, 51], possibly leading to larger d_μ and d_τ. In Section 4.3 and Section 4.4 we shall see how G2HDM gives rise to larger d_μ and d_τ, respectively, while still maintaining the possibility of yielding a smaller value should the bounds close in.

4.2 The Electron

For the electron, an extensive study of eEDM in G2HDM can be found in the 2018 [16] and 2020 [52] papers of Fuyuto, Hou, and Senaha. Our investigation on eEDM [53] is essentially an extension of the 2020 paper to a larger parameter space.

4.2.1 Cancellation Mechanism

As mentioned in Section 2.2, one big motivation for G2HDM as a viable model is the fact that $\mathcal{O}(1)\rho_{tt}$ can drive baryogenesis through $\lambda_t \mathrm{Im}\rho_{tt}$. However, this same ρ_{tt}, along with ρ_{ff} for a given fermion f, also generates EDM for said fermion (Section 3.2). We thus arive at a "point of tension" between theory and experiment: we desire a large ρ_{tt} for baryogenesis, but need a small ρ_{tt} to survive precision bounds on various EDMs. Electron EDM, in particular, is a great "observable of contention", since experiments measuring it are the most precise compared to other EDMs. In an attempt to address this issue, Fuyuto, Hou, and Senaha proposed a "cancellation ansatz" between ρ_{ee} and ρ_{tt}

$$\mathrm{Re}\rho_{ee} = -r\frac{\lambda_e}{\lambda_t}\mathrm{Re}\rho_{tt}, \quad \mathrm{Im}\rho_{ee} = +r\frac{\lambda_e}{\lambda_t}\mathrm{Im}\rho_{tt}, \tag{4.1}$$

which facilitates a "cancellation mechanism" that allows for small values of eEDM while keeping a *sizeable* ρ_{tt}. The "cancellation" in this mechanism arises from the opposite signs of the W-loop and the top-loop in the Barr-Zee diagrams. Referring to (3.11) and (3.19), we can see that

$$(d_l^{\phi G})_t = -\frac{e\, m_l}{(4\pi)^4}\sqrt{2}G_F \sum_{\phi=h,H,A}\sum_{G=\gamma,Z}(\rho \text{ couplings})(\text{Loop functions}) \tag{4.2}$$

$$(d_l^{\phi G})_W = +\frac{e\, m_l}{(4\pi)^4}\sqrt{2}G_F \sum_{\phi=h,H,A}\sum_{G=\gamma,Z}(\rho \text{ couplings})(\text{Loop functions}) \tag{4.3}$$

thus the effectiveness of such a cancellation is determined by the relationship between the new ρ couplings and the loop functions of the Barr-Zee diagrams. In the case of total cancellation, $(d_l^{\phi G})_t = -(d_l^{\phi G})_W$, which gives

$$\text{To be added} \tag{4.4}$$

which can be factored into a ρ-dependent part and a loop-function-dependent part r. Rearranging (4.4) thus gives us the form of the cancellation ansatz. This ansatz signifies two key points. First, it gives a flavor hierarchy $|\rho_{ee}|/|\rho_{tt}| \sim \lambda_e/\lambda_t$ that reflects SM. Second, it represents a phase lock between ρ_{ee} and ρ_{tt}. With our working assumption of Higgs masses, this ansatz results in a "dip" in eEDM around

the r value of ~ 0.7, which is when complete cancellation occurs between the W-loop and the top-loop. This provides a mechanism for the eEDM in G2HDM to be small and evade the experimental bounds while not directly modifying ρ_{tt}.

4.2.2 Enlarging the Parameter Space

When revisiting their study, we found the assumptions on the value of ρ_{tt} to be quite "conservative", setting $\mathrm{Re}\rho_{tt} = \mathrm{Im}\rho_{tt} = -0.1$ (which equates to $|\rho_{tt}| = 0.1\sqrt{2} \approx 0.14$). We believe that might be due to *playing it safe* under the pressure of the rapid advancements on the experimental front. In our study [53], we *push against the boundary*, and explore a larger range of ρ_{tt}, up to $\mathrm{Re}\rho_{tt} = \mathrm{Im}\rho_{tt} = -0.3$ ($|\rho_{tt}| = 0.3\sqrt{2} \approx 0.42$). We want to see how big we can keep the parameter space for baryogenesis while still satisfying precision constraints. As mentioned before, one of the key points of G2HDM is the *flavor hierarchy*, illustrated by the *rule of thumb* (2.2). This "cancellation ansatz" happens to capture the idea of such a hierarchy pretty well from a numerical standpoint; so, for the sake of numerical illustration of the flavor hierarchy, we extend the ansatz to all fermion ρ_{ff}s, except for the top itself:

$$\mathrm{Re}\rho_{ff} = -r\frac{\lambda_f}{\lambda_t}\mathrm{Re}\rho_{tt}, \quad \mathrm{Im}\rho_{ff} = +r\frac{\lambda_f}{\lambda_t}\mathrm{Im}\rho_{tt}. \tag{4.5}$$

We must reiterate that this is merely a move of convenience, and the actual values of the ρ_{ff}s need not precisely match this ansatz. Results are shown in Figure 4.1. For the sake of clarity, we have taken a slight liberty in illustrating the range of the purple "allowed window" band, using the left- and right-most curves instead of the left and right side of a given curve. Nevertheless, the trend we wish to describe is not affected by such. From our results, it can be seen that as $|\rho_{tt}|$ increases, the allowed window of the proportionality parameter r shrinks, yet there is still a decent range of acceptable probable values. $\mathrm{Re}\rho_{tt} = \mathrm{Im}\rho_{tt} = -0.1$ was indeed a conservative representative value, and $\mathrm{Re}\rho_{tt} = \mathrm{Im}\rho_{tt} = -0.3$ may still be a viable option in the baryogenesis parameter space.

4.3 The Muon

After the electron, we move on to its slightly heavier cousin, the muon. Since the bound on the muon is not as strong, one does not need to resort to the cancellation ansatz immediately. Instead, we perform a scan of the ρ_{tt} parameter space for a representative $\rho_{\mu\mu}$ value, and see how it affects the μEDM. Results are shown in Figure 4.2. We see that there is still a "cancellation dip" for the neutral scalar-attached loops, which arises from the opposite signs of the W-loop and the top-loop. The details of said cancellation is exactly the same as that of the electron. Our predicted values for μEDM are still two to three orders of magnitude below the current bounds, so we are eager to see development on the experimental front. Once the bounds close in, it may also be fruitful to consider the "cancellation ansatz" on the muon as well, especially since the leptons share a extra Yukawa matrix ρ^l, which makes it more likely that the ρ_{ll} might exhibit similar relationships with ρ_{tt}.

4.4 The Tau Lepton

Lastly, we analyze the heaviest lepton, the tau. On the experimental front, the precision of tau EDM (τEDM) measurements are still pretty low. We perform the same calculations as the muon, with $\rho_{\mu\mu} = i\lambda_\mu$ replaced by $\rho_{\tau\tau} = i\lambda_\tau$. Results are shown in Figure 4.3. As seen in the figure, our predicted values are still several orders of magnitude below current experimental results. Further precision or methodology improvements are required for a more fruitful analysis of τEDM, so we just present our results here without much further comment.

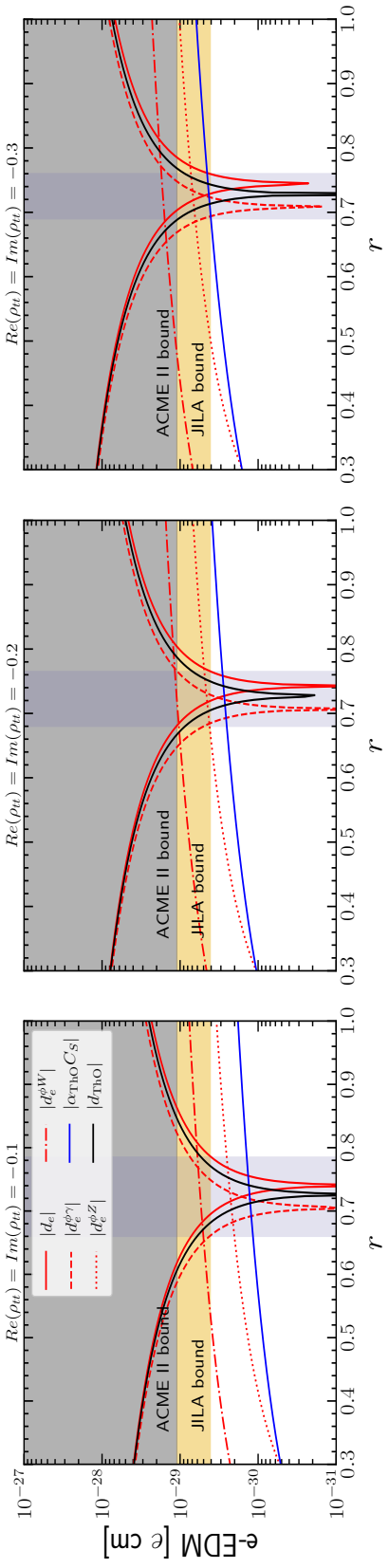

Figure 4.1: eEDM v.s. r for a larger range of ρ_{tt} with ansatz Eq. (4.5). ($c_\gamma = 0.1, m_{H,A,H^+} = 500\,\mathrm{GeV}$)

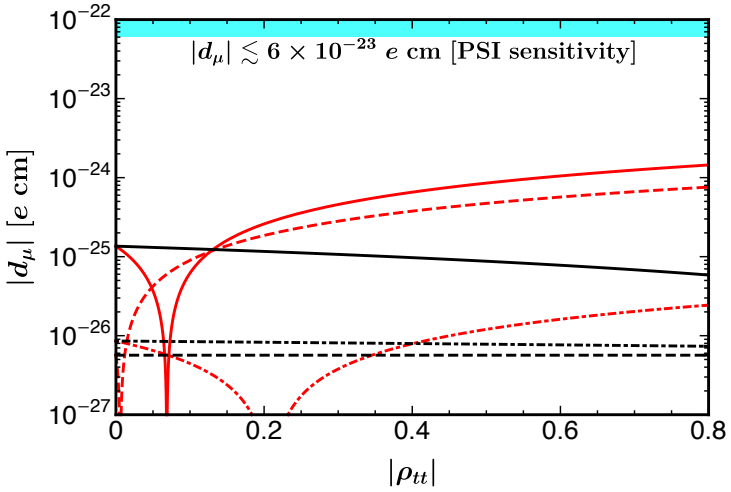

Figure 4.2: μEDM results.

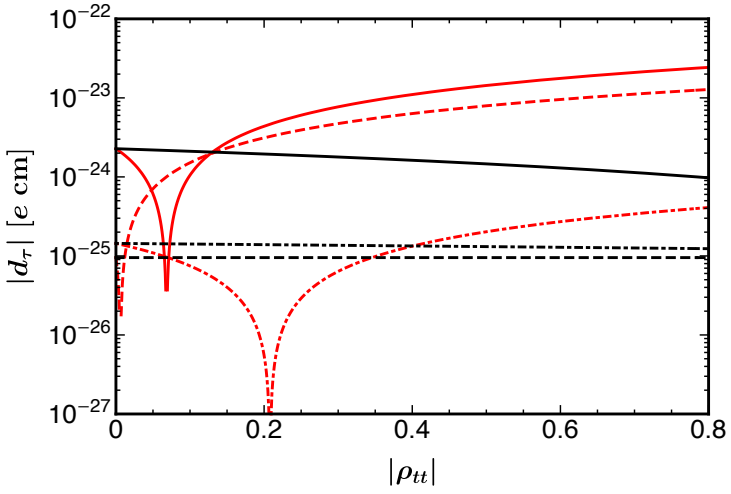

Figure 4.3: τEDM results.

Chapter 5

Electric and Chromo-electric Dipole Moment of Quarks

After the analysis for leptons, we turn our gaze towards EDMs involving quarks. However, since quarks are always confined as hadrons, it is extremely difficult, if not outright impossible, to directly probe the EDMs of individual quarks, given the state of current technology and our understanding of QCD. A quick literature [2] review shows that there are indeed no direct experimental observations for the EDMs of all the quarks lighter than the top quark. We comment on the situation of the top quark in Section 7.1.3. It is natural, under these circumstances, to shift our attention towards hadron EDMs, and utilize the EDM of hadrons to observe the effect of the EDMs of individual quarks. The prime candidate in this case would be the neutron EDM (nEDM).

5.1 The Neutron

5.1.1 Experimental Overview

Neutron EDM measurements have been in the experimental realm for quite some time already. The most recent results are given by PSI [54] in 2020, setting the

bound at $|d_n| < 1.8 \times 10^{-26}\ e\,\mathrm{cm}$. We can use the same back-of-the-envelope mass-scaling estimate that we did for the leptons to estimate the "equivalent precision" bound for nEDM from the eEDM bound. Since $m_u \sim m_e$ and m_d is barely 10 times greater than m_e, we can place the estimated nEDM value at $\sim 10^{-29}\ e\,\mathrm{cm}$. This places the current nEDM bound 3-4 orders of magnitude away.

Even though the nEDM experimental precision is not as good as that of the eEDM experiments, just looking at the numbers does invoke a *mild* sense of optimism, especially since this is a *very* naive estimate, as the dynamics involved in the neutron is much more complicated. One can reasonably expect the value to be suitably larger. Unfortunately, that optimistic feeling is quickly extinguished when we take a look at the progress over the past years. We cite here Figure 5.1, taken from the Snowmass conference report [1], as a good visual description of nEDM experimental progress. As can be seen from said figure, progress on the nEDM front has stagnated for a decade or so, with the precision plateauing at $\sim 10^{-26}\ e\,\mathrm{cm}$. However, we see a silver lining in the report: projects to improve the sensitivity, based on ultra-cold-neutron (UCN) methods, are already in the works. There is a follow-up project at PSI, named n2EDM [55], which plans to reach a sensitivity of $\sim 10^{-27}\ e\,\mathrm{cm}$ within a decade. Furthermore, there is a new experiment under construction at the Spallation Neutron Source [56] at Oak Ridge National Laboratory (ORNL), which projects a precision down to $10^{-28}\ e\,\mathrm{cm}$. Nevertheless, it is still worth to explore the nEDM parameter space, which is what we did [53].

5.1.2 G2HDM Calculations

As mentioned in the theory section, there are additional chromo-EDM and Weinberg term contributions to take into account that arise from the fact that quarks interact via QCD. To evaluate the combined combination of these contributions to nEDM, we use the more recent formula [57]

$$d_n = -0.20\, d_u + 0.78\, d_d + e\,(0.29\, \tilde{d}_u + 0.59 \tilde{d}_d) + e\, 23\ \mathrm{MeV}\, C_W \qquad (5.1)$$

instead of the widely cited classic review of Pospelov and Ritz [58]. We present the G2HDM-with-extended-ansatz (4.1)-applied calculation results for nEDM in Figure 5.2. Interestingly, our predictions for nEDM are not too far below the current experimental bound. We see that, even for $|\rho_{tt}| = 0.3\sqrt{2} \approx 0.42$, one can still survive the current PSI bound. The projected $\sim 10^{-27}\ e\,\mathrm{cm}$ sensitivity of n2EDM at PSI covers the range illustrated in Figure 5.2, putting stress on our model. Fortunately, there is still a possibility of lowering the predicted nEDM value of our model should the new experimental bounds indeed close in.

So far, we have been utilizing the "extended" cancellation ansatz (4.5) in our above calculations and analyses. However, we have to reiterate that it is merely a convenient way to numerically illustrate the *flavor hierarchy* of the G2HDM. A closer examination of the "extended" ansatz reveals a logical flaw: since ρ_{uu} and ρ_{tt} are in the same ρ matrix, and the ansatz obviously does not hold for ρ_{tt} itself, there is no reason to expect it to hold for ρ_{uu}. Thus, for this situation, we should fall back one step, and rely on the *rule of thumb* (2.2) instead of the ansatz. Hence, we relax the ansatz for ρ_{uu}, and explore the range of $\mathcal{O}(\lambda_u)$ by varying

$$|\rho_{uu}| \in [0.3\lambda_u, 3\lambda_u], \quad \arg\rho_{uu} \in [-\pi, \pi] \tag{5.2}$$

while keeping the other ρ_{ff}s intact, i.e. still following the ansatz. We present our results for said variation in Figure 5.3. The different colors of the points represent different values of $\arg\rho_{uu}$, and an interesting pattern can be seen among them. The red points have negative $\arg\rho_{uu}$, which is the same sign as ρ_{tt}; the nEDM of these points are larger, but stay mostly below the PSI bound. On the other hand, the blue points have *positive* $\arg\rho_{uu}$, which is the *opposite* sign as ρ_{tt}; remarkably, the value of nEDM of these points drop significantly, reaching as low as $10^{-28}\ e\,\mathrm{cm}$ or lower, evading even the projected sensitivity of n2EDM! This phenomenon in Figure 5.3 illustrates a *natural* cancellation mechanism present within the dynamics of nEDM, arising from the phase difference of ρ_{uu} and the other ρ_{ff}. Even though this mechanism can evade the projected n2EDM sensitivity, it can still be probed by the SNS at ORNL, with its down to $\sim 10^{-28}\ e\,\mathrm{cm}$ projected sensitivity. This

experiment may take more than a decade to come to fruition, but it almost fully covers our projected range, since the blue dots are still mostly concentrated above $10^{-28}\ e\,\mathrm{cm}$.

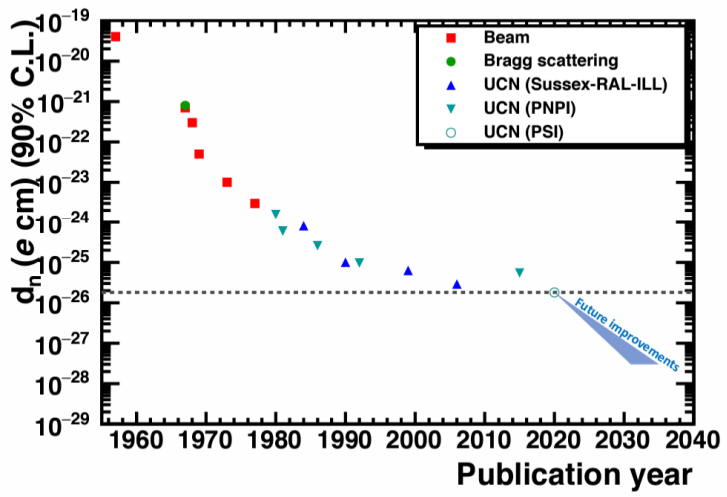

Figure 5.1: nEDM experimental progress [1]

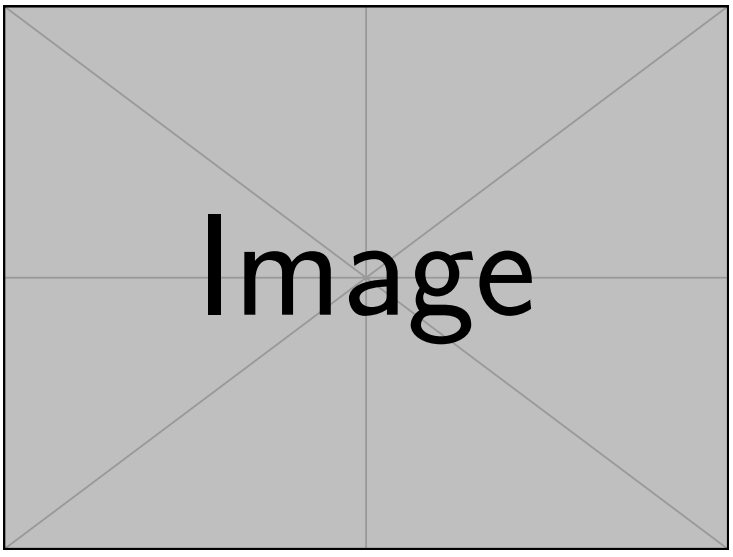

Figure 5.2: nEDM results with extended ansatz.

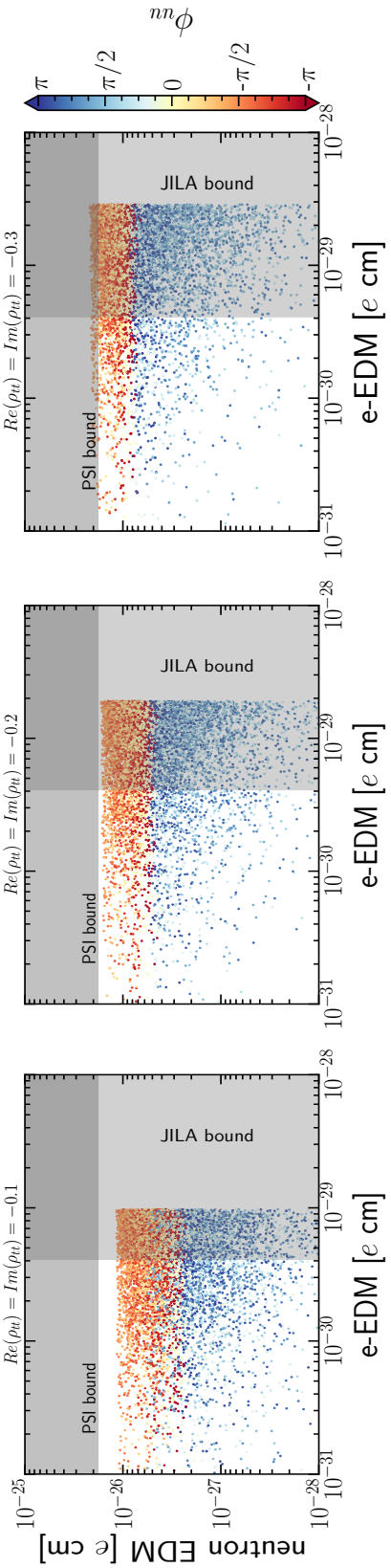

Figure 5.3: Results for eEDM and nEDM with $|\rho_{uu}| \sim \lambda_u$.

Chapter 6

Combined Analysis of eEDM and nEDM

In the previous two chapters, we saw that our G2HDM predictions for eEDM and nEDM lie either right on or slighly below their current respective experimental bounds. This strongly suggests that the combined results of these two observables will hold great significance, and is warrant of a combined analysis and discussion. We present combined results for eEDM and nEDM with the extended cancellation ansatz (4.5) in the range $r \in [0.6, 0.8]$ in Figure 6.1. The eEDM cancellation mechanism from Section 4.2.1 at $r \approx 0.7$ is clearly illustrated, while nEDM exhibits no obvious cancellation phenomena. If one were to isolate the EDM contributions of the individual up and down quarks, the ansatz-based cancellation would indeed occur seperately for each quark. However, the chromo-EDM and Weinberg diagram contributions do not exhibit this kind of cancellation, so there is no visible cancellation for nEDM. For the relaxed "order-of-magnitude" ρ_{uu}, we refer back to Figure 5.3. Since ρ_{uu} does not meaningfully contribute to d_e, the eEDM parameter space is not significantly affected by this relaxation of the ansatz. If one looks closely, one can see points of the same color forming the signature "cancellation dip" in the eEDM direction. This also elucidates that the *natural* cancellation in nEDM is a different mechanism from the *ansatz-based* cancellation

of eEDM.

To apply our theoretical predictions, we turn our gaze toward the eEDM and nEDM experiments. Given the recent rapid development on the eEDM experimental front, it is not unreasonable to expect an order-of-magnitude improvement in the coming decade. As mentioned in Section 5.1.1, n2EDM at PSI projects an order-of-magnitude increase in precision in the next decade, while SNS at ORNL projects a two-order-of-magnitude increase in precision in the next 20 years. This means that within the two decades to come, both the eEDM and nEDM experimental fronts will have enough precision to probe the vast majority of our respective predicted G2HDM parameter spaces. This puts G2HDM in the prime position for *discovery* in not one, but TWO precision fronts. One could even call that a *double whammy*! However, given the pretty specific conditions proposed for eEDM, resulting in a rather restrictive parameter space, one might deem our hope of discovery right around the current bound at 10^{-30}, or even 10^{-29}, to be wishful thinking. We would then refer you to the story of the discovery of $B_0 - \bar{B}_0$ mixing. In 1987, CLEO [59] published their bound on the strength of $B_0 - \bar{B}_0$. In that same year, ARGUS [60] announced their *discovery* of $B_0 - \bar{B}_0$ right on the CLEO bound. Thus, it is not unreasonable to expect an eEDM discovery in the vicinity of the current JILA bound.

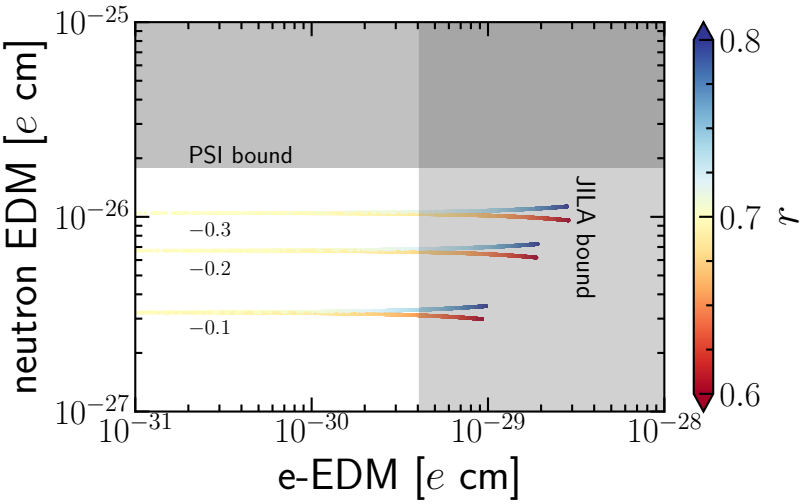

Figure 6.1: Combined eEDM-nEDM results.

Chapter 7

Conclusion

7.1 Comments

Before we reach the summary of this study, we want to comment on some unaddressed details.

7.1.1 Heavy Higgs Masses

Throughout the calculations in this study, we have assumed degeneracy of the exotic Higgses, either at 300 or 500 GeV. This has been done primarily to reduce the number of variables in the analysis, and focus on the effects of the extra Yukawa couplings on various EDMs. As a matter of fact, this assumption is actually two assumptions in one: the choice of benchmark mass value and the choice of imposing degeneracy. We would like to address the concequences of lifting/flexing each assumption seprately. First, regarding the choice of benchmark. For eEDM and nEDM, we have set the exotic Higgs masses to the higher value of 500 GeV. This leads to a smaller two-loop contribution to the EDMs, since the loop functions are dependent on and monotonically increasing with $m^2_{t/W}/m^2_{H/A/H^+}$. This also changes the exact r value where the cancellation occurs. However, at the same time, larger exotic Higgs masses lead to a less efficient scenario for baryogenesis. In a sense, this is the "conservative" benchmark, sacrificing baryogenesis efficiency

for some extra "headroom" in evading the EDM bounds. On the other hand, the 300 GeV mass value used in the μEDM and τEDM calculations is the "optimistic" benchmark, meant to explore the upper limits of the respective EDMs and see how close we are to the current experimental bounds. We have checked the eEDM and nEDM calculations at the 300 GeV benchmark and, unsurprisingly, the qualitative results are the same, with only the quantitative differences described above. Second, regarding the mass degeneracy. As mentioned in Section 3.2, with the degeneracy in place, one-loop effects are even further supressed. Lifting this degeneracy will increase the importance of the one-loop contribution, but unless the off-diagonal terms of the lepton ρ-matrix are large, which runs against our *flavor hierarchy* phenomenon, the two-loop effects will still be dominant by at least an order of magnitude or two. Also, nondegenerate exotic Higgs masses opens us up to the scrutiny of electroweak precision constraints [2], also known as oblique parameters[1]. This will require us to explore the scenarios of custodial symmetry $m_A = m_{H^+}$ and twisted-custodial symmetry [64] $m_H = m_{H^+}$. All in all, we can still enlarge the parameter space by varying the masses of the exotic Higgses, but we will have to deal with different constraints. We thus relegate a thorough investigation of the Higgs masses to further studies.

7.1.2 Muon $g-2$

During our analysis of μEDM and τEDM, the Fermilab Muon g-2 experiment reported [65] their first measurement of the muon anomalous magnetic moment $a_\mu = (g-2)_\mu$. Their result not only confirmed the old BNL result [66], but also put the combined experimental value at $a_\mu^{\text{Exp}} = 116\,592\,061(41) \times 10^{-11}$, which disagreed with the SM prediction [67] $a_\mu^{\text{SM}} = 116\,591\,810(43) \times 10^{-11}$ by more than 4σ,

$$a_\mu^{\text{Exp}} - a_\mu^{\text{SM}} = (251 \pm 59) \times 10^{-11}. \tag{7.1}$$

[1]The definition of these obilque parameters in the context of 2HDMs can be found in [61], while the explicit formulae for multi-Higgs models have been derived in [62, 63].

This was indeed a shock at that time, which prompted us to add in related discussions and analysis to our EDM study. As it is not the main point of *this* study, we refer you to section V of our paper [68] for detailed discussion, with a brief summary given here. Muon $g-2$ has main contributions in G2HDM from the one-loop diagram, so to accomodate the experimental result, one needs [69] very large $\rho_{\tau\mu}$ and $\rho_{\mu\tau}$, as well as sub-TeV *nondegenerate* m_H and m_A. This implies a near-perfect alignment $c_\gamma \to 0$ and a small ρ_{tt}. This in turn suppresses the two-loop contributions to all EDMs, while also makeing baryogenesis less favorable. Although the most recent experimental update [70] on this matter has strengthened the precision of the 2021 result, the other fronts do not look as optimistic. Recent lattice QCD results [71] are in tension with other relevant experimental results [72]; meanwhile, theorists are attempting [73] to reconcile the current theoretical situation. It remains to be seen how this "anomaly" will develop in the future.

7.1.3 Top Chromo-EDM

We would like to mention that the nEDM portion of this study was originally motivated by the ability of the LHC to probe top CPV through top chromo-EDM [74]. Probing the EDM and cEDM of the top quark directly would be ideal for direct exploration of the ρ_{tt} parameter space. Alas, the current bounds of the top cEDM are still relatively weak, so we shifted our gaze towards other hadronic EDMs and settled on nEDM, where the up and down cEDM come into play. Fortunately, we found rather good prospects for G2HDM in nEDM! We do hope that future improvements on the top cEDM measurement will come to fruition, and eagerly anticipate the insights it may bring in the realm of CPV and BAU.

7.2 Summary and Conclusion

In this thesis, we have analyzed various EDMs of fundamental particles in the framework of the General Two Higgs Doublet Model, a two-Higgs doublet model characterized by lack of Z_2 symmetry, *alignment* between the SM and exotic Higgs, and extra Yukawa couplings governed by *flavor hierarchy*.

We note that to evade precision bounds while satisfying the conditions for baryogenesis, a cancellation is possible, which is also an indicator of an underlying *flavor hierarchy*. This is most prevalent in eEDM, where bounds are the strongest, and experimental precision improving rapidly. We analyze μEDM, with our predictions still being a couple orders of magnitude below current experimental bounds. We present results for τEDM, but provide no further analysis since the bounds are still too imprecise. We analyze quark EDM through nEDM, and optain promising prospective results, especially when viewed together with eEDM. We stress that this is a noteworthy area to pay attention to in the upcoming decade or two.

The improved precision of the eEDM and nEDM experiments may shake up new discussion in the realm of CPV. If G2HDM is indeed the source of EWBG, the combined efforts of eEDM and nEDM experiments seem poised for major discovery, potentially a *double whammy*, in the upcoming decade or two. Along with direct searches for exotic Higgs at LHC, ongoing efforts at Belle II as well as other flavor frontiers, we might soon see whether we can unveil what Nature has laid out for baryogenesis.

References

[1] R. Alarcon *et al.*, "Electric dipole moments and the search for new physics," *arXiv preprint arXiv:2203.08103*, 2022. v, 32, 35

[2] R. L. Workman *et al.*, "Review of particle physics," *Progress of Theoretical and Experimental Physics*, vol. 2022, no. 8, 2022. 1, 31, 42

[3] M. Thomson, *Modern particle physics*. Cambridge, United Kingdom ; New York: Cambridge University Press, 2013. 2

[4] U. Sarkar, *Particle and astroparticle physics*, ser. Series in high energy physics, cosmology, and gravitation. New York: Taylor & Francis, 2008. 2

[5] A. R. Liddle, *An introduction to modern cosmology*, 3rd ed. Chichester, West Sussex: John Wiley and Sons, Inc., 2015. 2

[6] J. D. Barrow and M. S. Turner, "Baryosynthesis and the origin of galaxies," *Nature*, vol. 291, no. 5815, pp. 469–472, 1981. 2

[7] M. S. Turner, "Big band baryosynthesis and grand unification," *AIP Conference Proceedings*, vol. 72, no. 1, pp. 224–243, 1981. 2

[8] V. A. Kuzmin, V. A. Rubakov, and M. E. Shaposhnikov, "On anomalous electroweak baryon-number non-conservation in the early universe," *Physics Letters B*, vol. 155, no. 1-2, pp. 36–42, 1985. 2, 6

[9] A. G. Cohen, D. B. Kaplan, and A. E. Nelson, "Weak scale baryogenesis," *Physics Letters B*, vol. 245, no. 3-4, pp. 561–564, 1990. 2

[10] A. A. Penzias and R. W. Wilson, "A measurement of excess antenna temperature at 4080mc/s," *Astrophysical Journal*, vol. 142, no. 1, pp. 419–421, 1965. 2

[11] J. H. Christenson, V. L. Fitch, J. W. Cronin, and R. Turlay, "Evidence for 2π decay of k^0 meson," *Physical Review Letters*, vol. 13, no. 4, pp. 138–+, 1964. 2

[12] A. D. Sakharov, "Violation of cp invariance c asymmetry and baryon asymmetry of universe," *Jetp Letters-Ussr*, vol. 5, no. 1, pp. 24–+, 1967. 2

[13] G. R. Farrar and M. E. Shaposhnikov, "Baryon asymmetry of the universe in the minimal standard model," *Physical Review Letters*, vol. 70, no. 19, pp. 2833–2836, 1993. 3

[14] A. I. Bochkarev, S. V. Kuzmin, and M. E. Shaposhnikov, "Electroweak baryogenesis and the higgs boson mass problem," *Physics Letters B*, vol. 244, no. 2, pp. 275–278, 1990. 3, 7

[15] G. C. Branco *et al.*, "Theory and phenomenology of two-higgs-doublet models," *Physics Reports-Review Section of Physics Letters*, vol. 516, no. 1-2, pp. 1–102, 2012. 5

[16] K. Fuyuto, W. S. Hou, and E. Senaha, "Electroweak baryogenesis driven by extra top yukawa couplings," *Physics Letters B*, vol. 776, pp. 402–406, 2018. 6, 7, 8, 25

[17] G. 't HOOFT, "Computation of quantum effects due to a 4-dimensional pseudoparticle," *Physical Review D*, vol. 14, no. 12, pp. 3432–3450, 1976. 6

[18] F. R. Klinkhamer and N. S. Manton, "A saddle-point solution in the weinberg-salam theory," *Physical Review D*, vol. 30, no. 10, pp. 2212–2220, 1984. 6

[19] G. R. Farrar and M. E. Shaposhnikov, "Baryon asymmetry of the universe in the minimal standard model," *Physical Review Letters*, vol. 70, no. 19, pp. 2833–2836, 1993. 7

[20] S. Kanemura, Y. Okada, and E. Senaha, "Electroweak baryogenesis and quantum corrections to the triple higgs boson coupling," *Physics Letters B*, vol. 606, no. 3-4, pp. 361–366, 2005. 7

[21] P. Huet and A. E. Nelson, "Electroweak baryogenesis in supersymmetric models," *Physical Review D*, vol. 53, no. 8, pp. 4578–4597, 1996. 7

[22] J. M. Cline and K. Kainulainen, "New source for electroweak baryogenesis in the minimal supersymmetric standard model," *Physical Review Letters*, vol. 85, no. 26, pp. 5519–5522, 2000. 7

[23] P. A. R. Ade *et al.*, "2013 results. xvi. cosmological parameters," *Astronomy & Astrophysics*, vol. 571, 2014. 7

[24] C. W. Chiang, K. Fuyuto, and E. Senaha, "Electroweak baryogenesis with lepton flavor violation," *Physics Letters B*, vol. 762, pp. 315–320, 2016. 7

[25] D. J. Griffiths, *Introduction to electrodynamics*, 4th ed. Boston: Pearson, 2013. 11

[26] J. D. Jackson, *Classical electrodynamics*, 3rd ed. New York: Wiley, 1999. 11

[27] P. A. M. Dirac, "The quantum theory of the electron," *Proceedings of the Royal Society of London Series a-Containing Papers of a Mathematical and Physical Character*, vol. 117, no. 778, pp. 610–624, 1928. 12

[28] E. E. Salpeter, "Some atomic effects of an electronic electric dipole moment," *Physical Review*, vol. 112, no. 5, pp. 1642–1648, 1958. 12

[29] T. E. Chupp, P. Fierlinger, M. J. Ramsey-Musolf, and J. T. Singh, "Electric dipole moments of atoms, molecules, nuclei, and particles," *Reviews of Modern Physics*, vol. 91, no. 1, 2019. 12

[30] M. Nowakowski, E. A. Paschos, and J. M. Rodríguez, "All electromagnetic form factors," *European Journal of Physics*, vol. 26, no. 4, pp. 545–560, 2005. 13

[31] J. D. Bjorken and S. Weinberg, "Mechanism for nonconservation of muon number," *Physical Review Letters*, vol. 38, no. 12, pp. 622–625, 1977. 15

[32] S. M. Barr and A. Zee, "Electric-dipole moment of the electron and of the neutron," *Physical Review Letters*, vol. 65, no. 1, pp. 21–24, 1990. 15

[33] R. G. Leigh, S. Paban, and R. M. Xu, "Electric-dipole moment of electron," *Nuclear Physics B*, vol. 352, no. 1, pp. 45–58, 1991. 15

[34] D. Chang, W. Y. Keung, and J. Liu, "The electric-dipole moment of w-boson," *Nuclear Physics B*, vol. 355, no. 2, pp. 295–304, 1991. 15

[35] C. Kao and R. M. Xu, "Charged-higgs-loop contribution to the electric-dipole moment of the electron," *Physics Letters B*, vol. 296, no. 3-4, pp. 435–439, 1992. 15

[36] D. BowserChao, D. Chang, and W. Y. Keung, "Electron electric dipole moment from cp violation in the charged higgs sector," *Physical Review Letters*, vol. 79, no. 11, pp. 1988–1991, 1997. 15

[37] T. Abe, J. Hisano, T. Kitahara, and K. Tobioka, "Gauge invariant barr-zee type contributions to fermionic edms in the two-higgs doublet models," *Journal of High Energy Physics*, no. 4, 2016. 15

[38] S. Weinberg, "Larger higgs-boson-exchange terms in the neutron electric-dipole moment," *Physical Review Letters*, vol. 63, no. 21, pp. 2333–2336, 1989. 18

[39] T. S. Roussy *et al.*, "An improved bound on the electron's electric dipole moment," *Science*, vol. 381, no. 6653, pp. 46–50, 2023. 23, 24

[40] V. Andreev *et al.*, "Improved limit on the electric dipole moment of the electron," *Nature*, vol. 562, no. 7727, pp. 355–+, 2018. 23, 24

[41] G. W. Bennett *et al.*, "Improved limit on the muon electric dipole moment," *Physical Review D*, vol. 80, no. 5, 2009. 24

[42] R. Chislett, "The muon edm in the g-2 experiment at fermilab," *EPJ Web of Conferences*, vol. 118, p. 01005, 2016. 24

[43] M. Abe *et al.*, "A new approach for measuring the muon anomalous magnetic moment and electric dipole moment," *Progress of Theoretical and Experimental Physics*, vol. 2019, no. 5, 2019. 24

[44] Y. H. Ema, T. Gao, and M. Pospelov, "Improved indirect limits on muon electric dipole moment," *Physical Review Letters*, vol. 128, no. 13, 2022. 24, 25

[45] A. Adelmann *et al.*, "Search for a muon edm using the frozen-spin technique," *arXiv preprint arXiv:2102.08838*, 2021. 24

[46] K. Inami *et al.*, "An improved search for the electric dipole moment of the τ lepton," *Journal of High Energy Physics*, no. 4, 2022. 24, 25

[47] E. Kou *et al.*, "The belle ii physics book," *Progress of Theoretical and Experimental Physics*, vol. 2019, no. 12, 2019. 24, 25

[48] W. Bernreuther, L. Chen, and O. Nachtmann, "Electric dipole moment of the tau lepton revisited," *Physical Review D*, vol. 103, no. 9, 2021. 24, 25

[49] G. D'Ambrosio, G. F. Giudice, G. Isidori, and A. Strumia, "Minimal flavour violation: an effective field theory approach," *Nuclear Physics B*, vol. 645, no. 1-2, pp. 155–187, 2002. 25

[50] G. Hiller, K. Huitu, T. Rüppell, and J. Laamanen, "Large muon electric dipole moment from flavor?" *Physical Review D*, vol. 82, no. 9, 2010. 25

[51] A. Crivellin, M. Hoferichter, and P. Schmidt-Wellenburg, "Combined explanations of (-2) and implications for a large muon edm," *Physical Review D*, vol. 98, no. 11, 2018. 25

[52] K. Fuyuto, W. S. Hou, and E. Senaha, "Cancellation mechanism for the electron electric dipole moment connected with the baryon asymmetry of the universe," *Physical Review D*, vol. 101, no. 1, 2020. 25

[53] W. S. Hou, G. Kumar, and S. Teunissen, "Discovery prospects for electron and neutron electric dipole moments in the general two higgs doublet model," *Physical Review D*, vol. 109, no. 1, 2024. 25, 27, 32

[54] C. Abel *et al.*, "Measurement of the permanent electric dipole moment of the neutron," *Physical Review Letters*, vol. 124, no. 8, 2020. 31

[55] N. J. Ayres *et al.*, "The design of the n2edm experiment nedm collaboration," *European Physical Journal C*, vol. 81, no. 6, 2021. 32

[56] "Oak ridge national laboratory nedm web page." [Online]. Available: https://nedm.ornl.gov/ 32

[57] T. Abe, J. Hisano, T. Kitahara, and K. Tobioka, "Gauge invariant barr-zee type contributions to fermionic edms in the two-higgs doublet models," *Journal of High Energy Physics*, no. 1, 2014. 32

[58] M. Pospelov and A. Ritz, "Electric dipole moments as probes of new physics," *Annals of Physics*, vol. 318, no. 1, pp. 119–169, 2005. 33

[59] A. Bean *et al.*, "Limits on b0bbar0 mixing and taub0 taub+," *Physical Review Letters*, vol. 58, no. 3, pp. 183–186, 1987. 38

[60] H. Albrecht *et al.*, "Observation of b0-b-bar-0 mixing," *Physics Letters B*, vol. 192, no. 1-2, pp. 245–252, 1987. 38

[61] I. Maksymyk, C. P. Burgess, and D. London, "Beyond s, t, and u," *Physical Review D*, vol. 50, no. 1, pp. 529–535, 1994. 42

[62] W. Grimus, L. Lavoura, O. M. Ogreid, and P. Osland, "A precision constraint on multi-higgs-doublet models," *Journal of Physics G-Nuclear and Particle Physics*, vol. 35, no. 7, 2008. 42

[63] ——, "The oblique parameters in multi-higgs-doublet models," *Nuclear Physics B*, vol. 801, no. 1-2, pp. 81–96, 2008. 42

[64] J. M. Gérard and M. Herquet, "Twisted custodial symmetry in two-higgs-doublet models," *Physical Review Letters*, vol. 98, no. 25, 2007. 42

[65] B. Abi *et al.*, "Measurement of the positive muon anomalous magnetic moment to 0.46 ppm," *Physical Review Letters*, vol. 126, no. 14, 2021. 42

[66] G. W. Bennett *et al.*, "Final report of the e821 muon anomalous magnetic moment measurement at bnl -: art. no. 072003," *Physical Review D*, vol. 73, no. 7, 2006. 42

[67] T. Aoyama *et al.*, "The anomalous magnetic moment of the muon in the standard model," *Physics Reports-Review Section of Physics Letters*, vol. 887, pp. 1–166, 2020. 42

[68] W. S. Hou, G. Kumar, and S. Teunissen, "Charged lepton edm with extra yukawa couplings," *Journal of High Energy Physics*, no. 1, 2022. 43

[69] W. S. Hou, R. Jain, C. Kao, G. Kumar, and T. Modak, "Collider prospects for the muon g 2 in a general two -higgs -doublet model," *Physical Review D*, vol. 104, no. 7, 2021. 43

[70] D. P. Aguillard *et al.*, "Measurement of the positive muon anomalous magnetic moment to 0.20 ppm," *Physical Review Letters*, vol. 131, no. 16, 2023. 43

[71] S. Borsanyi *et al.*, "Leading hadronic contribution to the muon magnetic moment from lattice qcd," *Nature*, vol. 593, no. 7857, pp. 51–+, 2021. 43

[72] F. V. Ignatov *et al.*, "Measurement of the

$$e + e - - > \pi + \pi -$$

cross section from threshold to 1.2 gev with the cmd-3 detector," *Physical Review D*, vol. 109, no. 11, 2024. 43

[73] G. Colangelo *et al.*, "Prospects for precise predictions of a_μ in the standard model," *arXiv preprint arXiv:2203.15810*, 2022. 43

[74] A. Tumasyan *et al.*, "Search for cp violation using

$$\mathrm{t\bar{t}}$$

events in the lepton+jets channel in pp collisions at

$$\sqrt{s}$$

= 13 tev," *Journal of High Energy Physics*, vol. 2023, no. 6, p. 81, 2023. 43